LAWRENCE
LIVERMORE
NATIONAL
LABORATORY

LLNL-CONF-475799

An Adaptive Particle Filtering Approach to Tracking Modes in a Varying Shallow Ocean Environment

J. V. Candy

March 24, 2011

IEEE OCEANS'11
Santander, Spain
June 6, 2011 through June 9, 2011

An Adaptive Particle Filtering Approach to Tracking Modes in a Varying Shallow Ocean Environment

J. V. Candy, *Fellow, IEEE*

Abstract—**The shallow ocean environment is ever changing mostly due to temperature variations in its upper layers ($<$ 100m) directly affecting sound propagation throughout. The need to develop processors that are capable of tracking these changes implies a stochastic as well as an "adaptive" design. The stochastic requirement follows directly from the multitude of variations created by uncertain parameters and noise. Some work has been accomplished in this area, but the stochastic nature was constrained to Gaussian uncertainties. It has been clear for a long time that this constraint was not particularly realistic leading a Bayesian approach that enables the representation of *any* uncertainty distribution. Sequential Bayesian techniques enable a class of processors capable of performing in an uncertain, nonstationary (varying statistics), non-Gaussian, variable shallow ocean. In this paper adaptive processors providing enhanced signals for acoustic hydrophone measurements on a vertical array as well as enhanced modal function estimates are developed. Synthetic data is provided to demonstrate that this approach is viable.**

Index Terms—**model-based processor, sequential Bayesian processor, sequential Monte Carlo, particle filter.**

I. INTRODUCTION

The shallow ocean is an uncertain, ever changing, dispersive environment dominated by ambient and shipping noise as well as temperature fluctuations that alter sound propagation throughout. A processor is required to adapt to these environmental variations while simultaneously tracking modal functions. A possible solution to this problem is accomplished by developing a sequential Bayesian processor capable of providing a joint solution to the modal function tracking (estimation) and environmental adaptivity problem.

One basic approach to this problem is termed *model-based*. Incorporating a propagation model into a signal processing scheme has evolved over a long period of time where it was recognized that by embedding a physics-based representation can significantly improve the processing [1]-[5]. In ocean acoustics there are many problems of interest [6]-[15] governed by propagation models of varying degrees of sophistication.

Here we are interested in a shallow water environment characterized by a normal-mode model. The model-based approach offer a means of estimating various quantities of high interest, but it also provides a methodology to statistically evaluate its performance on-line [17].

In this paper, we are primarily interested in investigating the application of the so-called "next generation" of model-based signal processing algorithms, primarily the unscented Kalman filter (*UKF*) and the particle filter (*PF*) with the goal of analyzing their performance on pressure-field data synthesized from the well-known Hudson Canyon experiments performed on the New Jersey shelf [11], [12]. Recall that the *PF* is a sequential Markov chain Monte Carlo (MCMC) Bayesian processor capable of providing reasonable performance for a multimodal problem estimating a non-parametric representation of the posterior distribution [24]. On the other hand, the *UKF* is a unimodal processor capable of representing any single peaked distribution using a statistical linearization technique based on sigma points that deterministically characterize the posterior [24].

Background for the state-space representation of our problem is given in Section II leading to the formulation of the forward propagators. The design of the *BP* for a shallow ocean acoustic problem is discussed in Section III and the results are given where we compare processor performance. We summarize and discuss our results in the final section.

II. STATE-SPACE PROPAGATOR

For our ocean acoustic signal enhancement problem we assume a horizontally-stratified ocean of depth h with a *known* horizontal source range r_s and depth z_s and that the acoustic energy from a point source can be modeled as a trapped wave governed by the Helmholtz equation [9], [14]. The standard separation of variables technique and removing the time dependence leads to a set of ordinary differential equations, that is, we obtain a "depth only" representation of the wave equation which is an eigenvalue equation in z with

$$\frac{d^2}{dz^2}\phi_m(z) + \kappa_z^2(m)\phi_m(z) = 0,\ m = 1, \cdots, M \qquad (1)$$

whose eigensolutions $\{\phi_m(z)\}$ are the so called *modal functions* and κ_z is the wave number in the z-direction. These solutions depend on the sound speed profile, $c(z)$, and the boundary conditions at the surface and bottom as well as the corresponding *dispersion* relation given by

$$\kappa^2 = \frac{\omega^2}{c^2(z)} = \kappa_r^2(m) + \kappa_z^2(m), \qquad m = 1, \ldots, M \qquad (2)$$

where $\kappa_r(m)$ is the horizontal wave number associated with the m-th mode in the r direction and ω is the harmonic source frequency.

By assuming a known horizontal source range *a priori*, we obtain a range solution given by the Hankel function, $H_0(\kappa_r r_s)$ enabling the pressure-field to be represented by

$$p(r_s, z) = \sum_{m=1}^{M} \beta_m(r_s, z_s)\phi_m(z) \tag{3}$$

where p is the acoustic pressure; ϕ_m is the m^{th} modal function with the modal coefficient defined by

$$\beta_m(r_s, z_s) := q \ H_0(\kappa_r r_s) \ \phi_m(z_s) \tag{4}$$

for q is the source amplitude.

A. State-Space Model

The depth-only eigen-equation can easily be transformed to state-space form by defining the state vector of the m-th mode as

$$\phi_m(z) := \begin{bmatrix} \phi_m(z) \\ \frac{d}{dz}\phi_m(z) \end{bmatrix} = \begin{bmatrix} \phi_{m1}(z) \\ \phi_{m2}(z) \end{bmatrix} \tag{5}$$

Thus, we have for the m-th mode the following state (vector) equation as:

$$\frac{d}{dz}\phi_m(z) = \mathbf{A}_m(z)\phi_m(z) \tag{6}$$

for

$$\mathbf{A}_m(z) = \begin{bmatrix} 0 & 1 \\ -\kappa_z^2(m) & 0 \end{bmatrix} \tag{7}$$

Assuming that the ocean acoustic noise can be characterized by additive uncertainties, we can extend the deterministic state equation for the M-modes, that is, $\Phi(z) := [\phi_1(z)|\cdots|\phi_M(z)]^T$ leading to the following $2M$-dimensional Gauss-Markov representation of the model:

$$\frac{d}{dz}\phi(z) = \mathbf{A}(z)\phi(z) + \mathbf{w}(z) \tag{8}$$

where $\mathbf{w}(z) = [w_1 \ \ w_2 \ \ \ldots \ \ w_{2M}]^T$ is additive, zero-mean random noise. The system matrix $\mathbf{A}(z)$ is defined as

$$\mathbf{A}(z) = \begin{bmatrix} \mathbf{A}_1(z) & \cdots & 0 \\ \vdots & \ddots & \vdots \\ 0 & \cdots & \mathbf{A}_M(z) \end{bmatrix} \tag{9}$$

and the overall state vector is

$$\phi(z) = [\phi_{11} \ \ \phi_{12} \mid \phi_{21} \ \ \phi_{22} \mid \ \ \ldots \ \ \mid \phi_{M1} \ \ \phi_{M2}]^T \tag{10}$$

This leads to the $measurement$ equations, which we can write as

$$p(r_s, z) = \mathbf{C}^T(r_s, z_s)\phi(z) + v(z) \tag{11}$$

where

$$\mathbf{C}^T(r_s, z_s) = [\beta_1(r_s, z_s) \ \ 0 \mid \ \ \cdots \ \ \mid \beta_M(r_s, z_s) \ \ 0] \tag{12}$$

The random noise terms $\mathbf{w}(z)$ and $v(z)$ can be assumed Gaussian and zero-mean with respective covariance matrices, $\mathbf{R}_{ww}$ and $\mathbf{R}_{vv}$. The measurement noise ($v(z)$) can be used to represent the "lumped" effects of near-field acoustic noise field, flow noise on the hydrophone and electronic noise. The modal noise ($\mathbf{w}(z)$) can be used to represent the "lumped" uncertainty of sound speed errors, distant shipping noise, errors in the boundary conditions, sea state effects and ocean inhomogeneities that propagate through the ocean acoustic system dynamics (normal-mode model). These assumptions, with known model parameters lead to the optimal solution of the state estimation problem (Kalman filter) [18].

Since our array spatially samples the pressure-field discretizing depth, we choose to analogously discretize the differential state equations using a central difference approach for improved numerical stability, that is, from Eq. 1 we obtain the following set of difference equations for the m-th mode

$$\begin{aligned} \phi_{m1}(z_\ell) &= \phi_{m2}(z_{\ell-1}) \\ \phi_{m2}(z_\ell) &= -\phi_{m1}(z_{\ell-1}) + (2 - \triangle z_\ell^2 \kappa_z^2(m))\phi_{m2}(z_{\ell-1}) \end{aligned} \tag{13}$$

with each of the corresponding A-submatrices given by

$$\mathbf{A}_m(z) = \begin{bmatrix} 0 & 1 \\ & \\ -1 & 2 - \triangle z_\ell^2 \kappa_z^2(m) \end{bmatrix}; \quad m = 1, \cdots, M \tag{14}$$

B. Augmented State-Space Model

The "parametrically adaptive" processor evolves from this representation by defining a parameter set of interest. Since we are primarily interested in an environmentally adaptive processor, that is, a processor capable of adjusting its parameters to variations in the environment such as temperature, noise, etc. We choose to capture these changes by allowing the modal coefficients to vary. Therefore, we define the *parameter vector* as

$$\theta_m(r_s, z_s) := \beta_m(r_s, z_s); \ \ m = 1, \cdots, M$$

and a new "augmented" state vector as

$$\Phi_m(z_\ell; \theta_m) := \Phi_m(z_\ell) = [\phi_{m1}(z_\ell) \ \phi_{m2}(z_\ell) \mid \theta_m(z_\ell)]^T$$

With this choice of parameters (modal coefficients) the augmented state equations for the m-th mode become

$$\begin{aligned} \phi_{m1}(z_\ell) &= \phi_{m2}(z_{\ell-1}) + w_{m1}(z_{\ell-1}) \\ \phi_{m2}(z_\ell) &= -\phi_{m1}(z_{\ell-1}) + (2 - \triangle z_\ell^2 \kappa_z^2(m))\phi_{m2}(z_{\ell-1}) \\ &+ \ w_{m2}(z_{\ell-1}) \\ \theta_m(z_\ell) &= \theta_m(z_{\ell-1}) + w_{\theta_m}(z_{\ell-1}) \end{aligned} \tag{15}$$

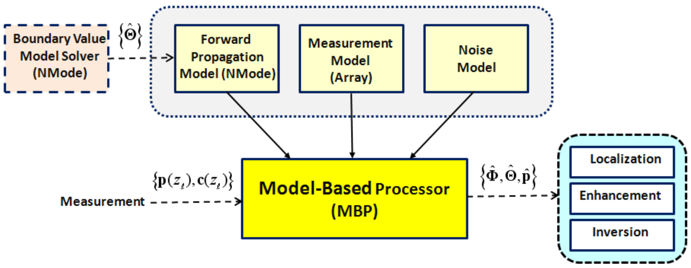

Fig. 1. Model-based processor design: (a) Boundary Solver for initial parameters. (b) Propagator, measurement and noise models. (c) *BP*. (d) Applications: localization, enhancement (tracking) and inversion.

where we have selected a *random walk* model ($\dot{\theta}_m(z) = w_{\theta_m}(z)$) to capture the variations of the modal coefficients with additive, zero-mean, Gaussian noise of covariance $R_{w_{\theta_m} w_{\theta_m}}$.

The random walk model can provide constraints in the simulation, since the parameter is modeled as Gauss-Markov implying that 95% of the samples must lie within confidence limits controlled by ($\pm 1.96\sigma_{m,m}$). This constitutes a *soft* statistical constraint of the parameter variations [16]. For our runs, we choose to start the processor with initial parameter estimates close to those values other researchers have meticulously estimated from the Hudson Canyon data set [11], [12].

More succinctly, for the m-th mode we can write

$$\Phi_m(z_\ell) = \mathbf{A}_m(z_{\ell-1})\Phi_m(z_{\ell-1}) + \mathbf{w}_m(z_{\ell-1}) \tag{16}$$

for

$$\mathbf{A}_m(z_{\ell-1}) = \left[\begin{array}{ccc|c} 0 & & 1 & 0 \\ -1 & & 2 - \triangle z_{\ell-1}^2 \kappa_z^2(m) & 0 \\ \hline 0 & & 0 & 1 \end{array}\right]$$

The corresponding measurement model is given by

$$p(r_s, z_\ell) = \sum_{m=1}^{M} \theta_m(z_\ell)\phi_m(z_\ell) + v(z_\ell);\ \ \ell = 1, \cdots, L \tag{17}$$

with dispersion (sound-speed)

$$c(z_\ell) = \frac{\omega}{\sqrt{\kappa_z^2(m) + \kappa_r^2(m)}},\ \ m = 1, \cdots, M;\ \ \ell = 1, \cdots, L \tag{18}$$

This completes the section on the discrete state-space representation of the shallow ocean acoustic (normal-mode) propagation model that is embedded as a "forward propagator" into the subsequent processors for signal enhancement. Note that the initial model parameters are obtained from the prior solution of the boundary value problem as shown in Fig. 1.

III. Processors

In this section we briefly develop the processors for our problem with details available in [24]. The basic adaptive problem we pursue in this paper can now be defined in terms of our mathematical models as:

GIVEN a set of noisy pressure-field and sound speed measurements varying in depth, $[\{p(r_s, z_\ell)\}, \{c(z_\ell)\}]$ along with the underlying state-space model of Eqs. 16, 17 and 18 with unknown modal coefficients, FIND the "best" (minimum error variance) estimate of the modal functions, that is, $\{\hat{\phi}_m(z_\ell|z_\ell)\}, \{\hat{\theta}_m(z_\ell|z_\ell)\}; m = 1, \cdots, M$ and measurements (enhanced) $\{\hat{p}(r_s, z_\ell)\}$.

We will primarily focus on the particle filter processor, since the unscented Kalman filter has been discussed elsewhere [18],[24] in detail. A particle filter is a different approach to nonlinear filtering in that it removes the restriction of additive Gaussian noise sources and is clearly capable of characterizing multimodal distributions. In fact, it might be easier to think of the *PF* as a histogram or kernel density like estimator in the sense that it is an empirical probability mass function (*PMF*) that approximates the desired posterior distribution such that statistical inferences can easily be performed and statistics extracted directly. The computational burden of the *PF* is much higher than that of the KF, since it must provide an estimate of the underlying state posterior distribution component-by-component at *each* z_ℓ-step along with the fact that the number of samples to characterize the distribution is equal to the number of particles.

$$\hat{\Pr}[\phi(z_\ell)|P_z] = \sum_{i=1}^{N_p} \mathcal{W}_i(z_\ell)\delta\big(\phi(z_\ell) - \phi_i(z_\ell)\big) \quad \forall z_\ell \tag{19}$$

$W_i(z_\ell)$ $\propto \hat{\Pr}[\phi_i(z_\ell)|P_z]$ is the estimated weights at depth z_ℓ;
$\phi_i(z_\ell)$ is the i-th particle at depth z_ℓ;
$\hat{\Pr}[\cdot]$ is the estimated empirical posterior distribution;
P_z is the set of batch pressure-field measurements, $P_z = \{p(r_s, z_1) \cdots p(r_s, z_L)\}$.

Thus, we see that once the underlying posterior is available, the estimates of important statistics can be extracted directly. For instance, the maximum a posteriori (*MAP*) estimate is simply found by locating a particular particle $\hat{\phi}_i(z_\ell)$ corresponding to the maximum of the *PMF*, while the conditional mean or equivalently the minimum mean-squared error (*MMSE*) estimate is calculated by integrating the posterior [24].

There are a variety of *PF* algorithms available, but perhaps the simplest is the *bootstrap* technique [24] which we apply to our problem. The *PF* design for our problem using the bootstrap approach requires the conditional state transition probability, $\Pr[\Phi(z_\ell)|\Phi(z_{\ell-1})]$, and the likelihood (probability) $\Pr[p(r_s, z_\ell)|\Phi(z_\ell)]$. Here the state transition is characterized by the underlying augmented state-space model for *each* mode. For the bootstrap implementation, we need only draw noise samples from the state and parameters distributions and use the dynamic models above (normal-mode/random walk) to generate the set of particles, $\{\Phi_{mi}(z_\ell)\}$ for each $i = 1, \cdots, N_p$.

The likelihood, on the other hand, is determined from the nonlinear pressure-field measurement model of Eq. 17, that is, for each mode we have

$$p_{mi}(r_s, z_\ell) := \theta_{mi}(z_\ell)\phi_{mi}(z_\ell) + v(z_\ell), \text{ for } \ell = 1, \cdots, L \quad (20)$$

and therefore the scalar likelihood (assuming Gaussian noise) is

$$\Pr[p(r_s, z_\ell)|\Phi(z_\ell)] = \frac{1}{\sqrt{2\pi R_{vv}}} \times \exp\left\{ -\frac{1}{2R_{vv}} \left(p(r_s, z_\ell) - \sum_{m=1}^{M} \theta_{mi}(z_\ell)\phi_{m1}(z_\ell; i) \right)^2 \right\} \quad (21)$$

Thus, we estimate the posterior distribution using a sequential Monte Carlo approach and construct a *bootstrap particle filter* [19]-[24] using the following steps:

- Initialize: $\Phi_m(0), w_{z_\ell} \sim \mathcal{N}(0, R_{ww}), W_i(0) = 1/N_p; i = 1, \cdots, N_p$;
- State Transition: $\Phi_m(z_\ell) = \mathbf{A}_m(z_{\ell-1})\Phi_m(z_{\ell-1}) + \mathbf{w}_m(z_{\ell-1})$;
- Likelihood Probability: $\Pr[p(r_s, z_\ell)|\Phi(z_\ell)]$;
- Weights: $W_i(z_\ell) = W_i(z_{\ell-1}) \times \Pr[\Phi_m(z_\ell)|\Phi_m(z_{\ell-1})]$;
- Normalize: $\mathcal{W}_i(z_\ell) = \frac{W_i(z_\ell)}{\sum_{i=1}^{N_p} W_i(z_\ell)}$;
- Resample: $\tilde{\Phi}_i(z_\ell) \Rightarrow \Phi_i(z_\ell)$;
- Posterior: $\hat{\Pr}[\Phi_m(z_\ell)|P_z] = \sum_{i=1}^{N_p} \mathcal{W}_i(z_\ell)\delta(\phi(z_\ell) - \phi_i(z_\ell))$; and
- *MAP* Estimate: $\hat{\Phi}_i^{MAP}(z) = \max_i \hat{\Pr}[\phi_i(z_\ell)|P_z]$;
- *MMSE* Estimate: $\hat{\Phi}_i^{MMSE}(z) = \frac{1}{N_p} \sum_{i=1}^{N_p} \mathcal{W}_i(z_\ell)\phi_i(z_\ell)$

More details can be found in the referenced textbooks and papers [19]-[24].

IV. MODEL-BASED OCEAN ACOUSTIC PROCESSING

In this section we discuss the development of the propagators for the Hudson Canyon experiment performed in 1988 in the Atlantic with the primary goal of investigating acoustic propagation (transmission and attenuation) using continuous wave data [11], [12]. The Hudson Canyon is located off the coast of New Jersey in the area of the Atlantic Margin Coring project borehole 6010 . The seismic and coring data are combined with sediment properties measured at that site. Excellent agreement was determined between the model and data indicating a well-known, well-documented shallow water experiment with bottom interaction and yielding ideal data sets for investigating the applicability of a *BP* to measured ocean acoustic data [11], [12]. The experiment was performed at low frequencies (50-600Hz) in shallow water of 73m depth during a period of calm sea state. A calibrated acoustic source was towed at roughly 36m depth along the 73m isobath radially to distances of 4 to 26Km. The ship speed was between 2 and 4Kts. The fixed vertical hydrophone array consisted of 24 phones spaced 2.5m apart extending from the seafloor up to a depth of about 14m below the surface. The normalized horizontal wave number spectrum for a 50Hz temporal frequency is dominated by 5 modes occurring at wave numbers between 0.14 to 0.21 m^{-1} with relative amplitudes increasing with increased wave number. A SNAP [13] simulation was performed and the results agree quite closely, indicating a well-understood ocean environment.

In order to construct the state-space propagator, we require the set of parameters which were obtained from the experimental measurements and processing (wave number spectra). The horizontal wave number spectra were estimated using synthetic aperture processing [11]. Eight temporal frequencies were employed: four on the inbounds (75Hz, 275Hz, 575Hz, 600Hz) and four on the outbound (50Hz, 175Hz, 375Hz, 425Hz). In this application we will confine our investigation to the 50Hz case, which is well-documented, and to horizontal ranges from 0.5-4Km. The raw measured data was processed (sampled, corrected, filtered, etc.) and supplied for this investigation.

A. Adaptive PF Design

The design and development of the environmentally adaptive *PF* proceeds through the following steps as shown in Fig. 2: (1) pre-processing the raw experimental data; (2) solving the boundary value problem (*BVP*) [9] to obtain initial parameter sets for each temporal frequency (e.g. wavenumbers, modal coefficients, initial conditions, etc.); (3) state-space forward propagator simulation of synthetic data for *PF* analysis/design; (4) application to measured data; and (5) *PF* performance analysis.

Pre-processing of the measured pressure-field data follows the usual pattern of filtering, outlier removal and Fourier transforming to obtain the complex pressure-field as a function of depth along the array. This data along with experimental conditions (frequencies, sound-speed profiles (CTD measurements), boundary conditions, horizontal wavenumber estimators (see [12] for details) provide the input to the normal mode *BVP* solutions (SNAP [6], KRACKEN [7], etc.) yielding the output parameters. These parameters are then used as input to the state-space forward propagator (see Fig. 2) developed in Sec. II.

The state-space propagator is then used to develop a set of synthetic pressure-field data with higher resolution than the original raw data, that is, a 46-element array at half-wave inter-element spacing rather than the 23-element array

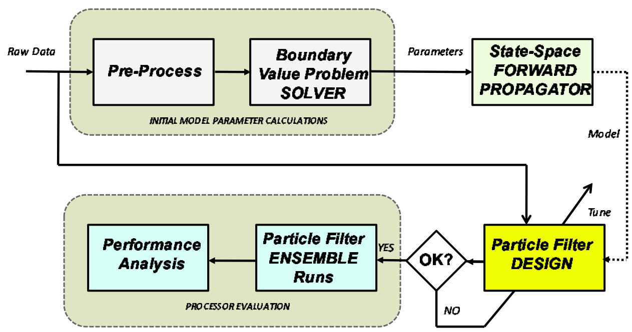

Fig. 2. *PF* design/development procedure: (a) Initial parameters/conditions. (b) Design runs. (c) Ensemble runs.

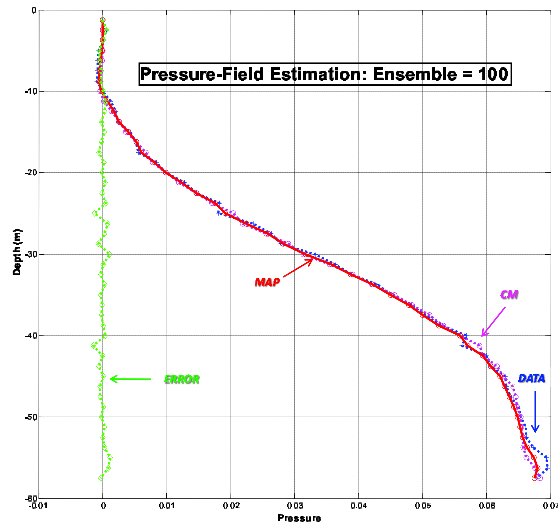

Fig. 3. Synthesized/enhanced pressure-field (blue dots) data from the Hudson Canyon experiment simulation with a 46-element hydrophone vertical array using particle filter estimators: *MAP* (red), conditional mean (*CM*) in magenta and the *UKF* (turquoise) with corresponding innovations (residuals) sequence (green).

used in the experiment. This set represents the "truth" data that can be investigated when "tuning" the *PF* (e.g. number of particles, covariances, etc.). Once tuned, the processors are applied directly to the measured pressure-field data (23-elements) after re-adjusting some of the processor parameters (covariances). Here the metrics are estimated and processor performance analyzed. Since each run of the *PF* is a random realization, that is, the process noise inputs are random, an ensemble of results are estimated with ensemble statistics presented. In this way, we can achieve a detailed analysis of the processor performance prior to fielding and operational version. In this paper we constrain our discussion results to processing synthesized pressure-field measurements using a 46-element array.

B. Results

First we investigate the enhancement capabilities of the *PF* in estimating the pressure-field over a 100-member ensemble shown in Fig. 3. Using 1000-particles, we see the synthesized data (dotted blue line) as well as both maximum a-posteriori (*MAP*) estimates (solid red line) and conditional mean (*CM*) estimates (dotted magenta line with circles). Both estimators appear to track the field quite well. The corresponding innovations (residual) sequence is also shown (green). Classically, both estimators produced satisfactory zero-mean/statistical whiteness tests as well as the *WSSR* tests indicating a "tuned" processor [18], that is, *PF*-(ZM-WT: $3\times10^{-4} < 3.5\times10^{-1}/9.4\%$ out/*WSSR* below) and *CM*-(ZM-WT: $1.5\times10^{-4} < 3.5\times10^{-1}/0.0\%$ out/*WSSR* below). The *UKF* processor also produced reasonable results: *UKF*-(ZM-WT: $1.5\times10^{-4} < 3.5\times10^{-1}/6.5\%$ out/*WSSR* below) for the enhanced pressure-field.

Ensemble mode tracking results are shown in Figs. 4 and 5 for each of the modal function estimators, the *PF* (*MAP/CM*) and the *UKF*. In Fig. 4 we observe that the performance of the *PF* (*MAP/CM*) appears to track the modes quite well especially compared to the *UKF*. The *PF* estimators perform equivalently. Two of the modal function estimates (first two) exhibit the largest errors as shown in Fig. 5 while the final three functional estimates are much better. The mean-squared (modal tracking) error for each mode is quite reasonable: *MSE*: $(222, 23, 5.5, 3.9, 3.7)\times10^{-9}$ again confirming the difficulty the estimator is having to maintain track on the two lower order modal functions. It is interesting to note that the modal coefficient estimates are constantly being adapted (adjusted) by the processor throughout the runs attesting to the nonstationary nature of the ocean statistics as illustrated in Fig. 6.

We also illustrate the multimodal aspect of the oceanic data by observing the modal function posterior *PDF* estimates for modes 1 and 5 as illustrated in Fig. 7. It is clear from the plots that for each depth multiple peaks appear in the posterior estimates. A slice of this probability surface at depth slice 10 shows just how the particles are allocated by the processor to estimate the various peaks in each *PDF* as shown in Fig. 8.

The pressure-field posterior is better behaved almost producing a near unimodal posterior for the predicted field. Visualizing a peak at each depth produces a "smooth" estimate (*MAP*) as shown in Fig. 8. This completes the analysis of the Hudson Canyon experimental data and the *PF* processing performance.

V. SUMMARY

In this paper we have developed on-line, adaptive, model-based solutions to the ocean acoustic signal processing problem based on the normal-mode propagation model and a vertical sensor array measurement system modeled after the Hudson Canyon experiment with a synthesized 46-element

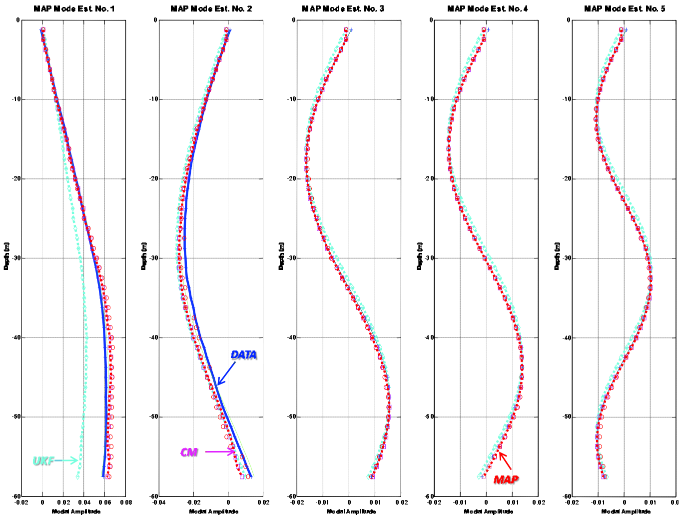

Fig. 4. Modal function tracking (estimation): synthesized Hudson Canyon data of a 46-element array (blue plus), *UKF* (turquoise dots), *MAP* (red circles) and *CM* (magenta squares) particle filters.

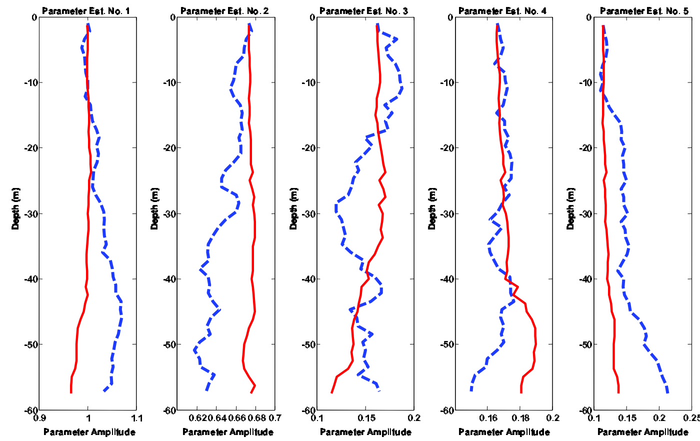

Fig. 6. Adaptive modal coefficient parameter estimates from the Hudson Canyon 46-element array simulation using the *MAP* (red) particle filter.

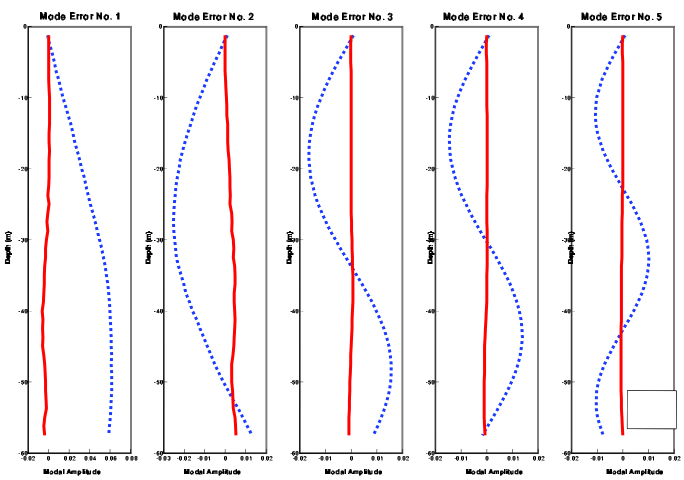

Fig. 5. Modal function tracking errors: synthesized Hudson Canyon data (blue plus) and *MAP* (red circles) particle filters errors.

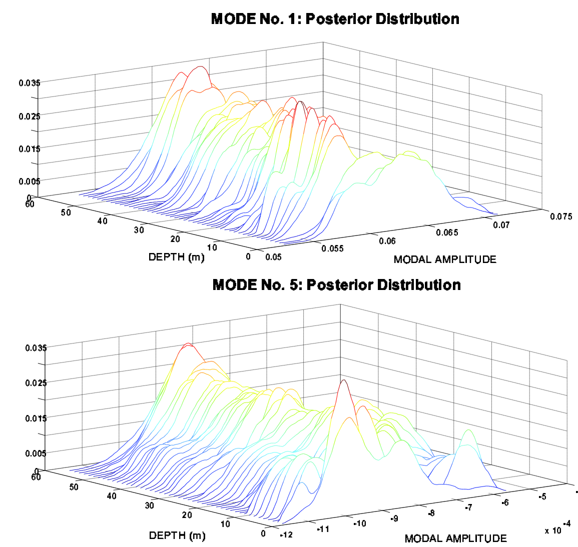

Fig. 7. *PMF* posterior estimation (modes 1 and 5) surfaces for synthesized Hudson Canyon 46-element array data (particle vs. time vs. probability).

vertical array. The algorithms employed were the unscented Kalman filter and the particle filter both modern approaches applied to this problem. We compared their performances and found slightly better performance of the *PF* over a 100-member ensemble. Our future efforts will be focused on extending the processors to actual measurement data.

Acknowledgments

This work performed under the auspices of the U.S. Department of Energy by Lawrence Livermore National Laboratory under Contract DE-AC52-07NA27344.

References

[1] M. J. Hinich, "Maximum likelihood signal processing for a vertical array," *J. Acoust. Soc. Am.*, **54**, 499-503, 1973.

[2] C. S. Clay, "Use of arrays for acoustic transmission in a noisy ocean," *Res. Geophys.*, **4**, (4), 475-507, 1966.

[3] H. P. Bucker, "Use of calculated sound fields and matched-field detection to locate sound in shallow water," *J. Acoust. Soc. Am.*, **59**, 329-337, 1976.

[4] A. M. Richardson, and L. W. Note, "A posteriori probability source localization in an uncertain sound speed, deep ocean environment," *J. Acoust. Soc. Am.*, **89**, (6), 2280-2284, 1991.

[5] E. J. Sullivan and D. Middleton, "Estimation and detection issues in matched-field processing", *IEEE J. Oceanic Eng.*, **18**, (3), 156-167, 1993.

[6] F. B. Jensen and M. C. Ferla, "SNAP: the SACLANTCEN normal-model propagation model," *Report SM-121*, Italy: SACLANTCEN, 1979.

[7] M. B. Porter, "The KRACKEN normal mode program," *Report SM-245*, Italy: SACLANTCEN, 1991.

[8] H. Schmidt, "SAFARI: Seismo-acoustic fast field algorithm for range independent environments," *Report SM-245*, Italy: SACLANTCEN, 1987.

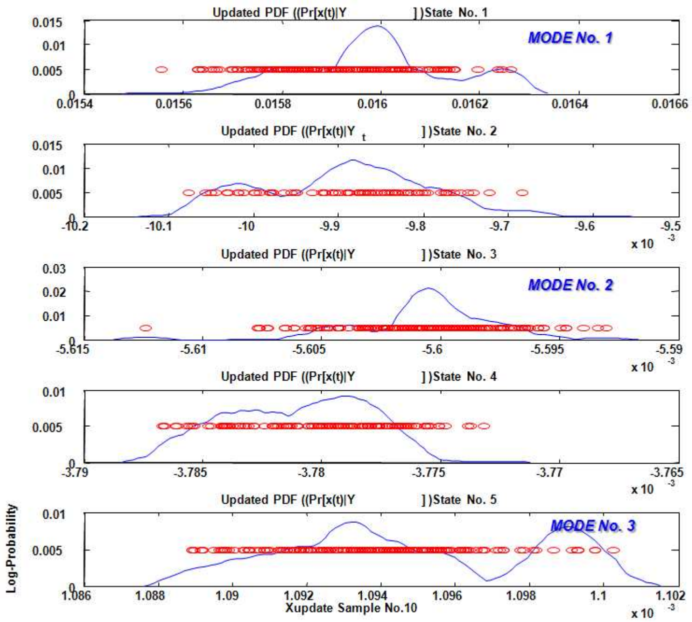

Fig. 8. Modal function posterior *PMF* estimation surface slice ($z = 10m$) for synthesized Hudson Canyon data (particle vs. probability for 1000-particles.

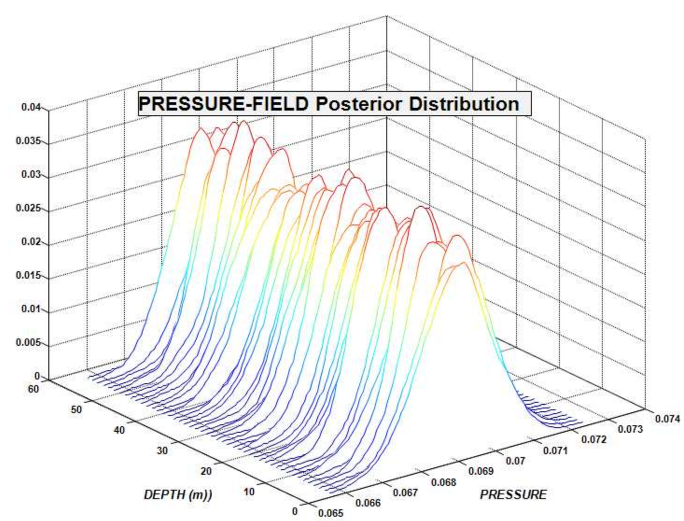

Fig. 9. Pressure-field posterior *PMF* estimation surface for synthesized Hudson Canyon data (particle vs. time vs. probability.

[9] F. B. Jensen, Kuperman, W. A., Porter M. B.,and H. Schmidt, *Computational Ocean Acoustics* New York: Amer. Instit. Physics Press, 1994.

[10] J. V. Candy and E.J. Sullivan. "Model-based processor design for a shallow water ocean acoustic experiment", *J. Acoust. Soc. Am.*, **95**, (4) 2038-2051, 1994.

[11] W. M. Carey, J. Doutt, R. Evans and L. Dillman, "Shallow water transmission measurements taken on the New Jersey continental shelf," *IEEE J. Oceanic Eng.*, **20**, (4), 321-336, 1995.

[12] A. R. Rogers, Y. Yamamoto and W. Carey, "Experimental investigation of sediment effect on acoustic wave propagation in shallow water," *J. Acoust. Soc. Am.*, **93**,1747-1761, 1993.

[13] F. B. Jensen, and M.C. Ferla, "SNAP: the SACLANTCEN normal-mode acoustic propagation model," *SACLANTCEN Report*,

[14] C. S. Clay, and H. Medwin, *Acoustical Oceanography*. New York:Wiley, 1977.

[15] J. V. Candy and E. J. Sullivan. "Ocean acoustic signal processing: a model-based approach." *J. Acoust. Soc. Am.*, **92**, (12), 3185-3201, 1992.

[16] J. V. Candy and E. J. Sullivan. "Model-based identification: an adaptive approach to ocean-acoustic processing." *IEEE Trans. Ocean. Engr.*, Vol. 21, No. 3, 273-289, 1996.

[17] A. Jazwinski, *Stochastic Processes and Filtering Theory*. New York:Academic Press, 1970.

[18] J. V. Candy, *Model-Based Signal Processing*. Hoboken, N.J.:Wiley/IEEE Press, 2006.

[19] B. Ristic, S. Arulampalam and N. Gordon, *Beyond the Kalman Filter: Particle Filters for Tracking Applications*, Boston: Artech House, 2004.

[20] O. Cappe, E. Moulines and T. Ryden, *Inference in Hidden Markov Models*, New York: Springer-Verlag, 2005.

[21] S. Godsill and P. Djuric, "Special Issue: Monte Carlo methods for statistical signal processing." *IEEE Trans. Signal Proc.*, vol. **50**, 2002.

[22] P. Djuric, J. Kotecha, J. Zhang, Y. Huang, T. Ghirmai, M. Bugallo and J. Miguez, "Particle Filtering," *IEEE Signal Proc. Mag.* vol. **20**, No. 5, 19-38, 2003.

[23] S. Haykin and N. de Freitas, "Special Issue: Sequential state estimation: from Kalman filters to particle filters." *Proc. IEEE*, vol. **92**, No. 3, 399-574, 2004.

[24] J. V. Candy, *Bayesian Signal Processing: Classical, Modern and Particle Filtering Methods*. Hoboken, N.J.:Wiley/IEEE Press, 2009.